

# Cyclostationary Feature Detector Experiments using Reconfigurable BEE2

Artem Tkachenko, Danijela Cabric, and Robert W. Brodersen  
Berkeley Wireless Research Center, University of California, Berkeley  
{artemtk, danijela, rb}@eecs.berkeley.edu

**Abstract**—This paper presents a comprehensive characterization of cyclostationary feature detectors through theoretical analysis, hardware implementation, and real-time performance measurements. Results of our study show that feature detectors are highly susceptible to sampling clock offsets. We propose a new detector that overcomes this limitation, and characterize its performance through experiments. In addition, the comparison with a conventional energy detector shows that feature detectors are more robust to adjacent channel interference.

## I. INTRODUCTION

Cyclostationary feature detectors have been introduced as a complex two dimensional signal processing technique for recognition of modulated signals in the presence of noise and interference [1]. Recently, they have been proposed for the detection of weak primary user signals in the context of spectrum sensing for cognitive radios. However, there are number of issues that must be addressed in order to understand the robustness of this technique in a new application.

In this paper we take a three phase approach in tackling some of the fundamental theoretical and practical questions for spectrum sensing. First, we model real system impairments and analyze their effects on feature detector theoretically. Then, we implement the proposed detectors on the real-time wireless testbed and investigate their low complexity implementations. Lastly, we use the testbed to characterize performance of feature detectors for the weak signal detection. We also compare them with a conventional energy detector.

The paper is organized as follows: Section 2 provides theoretical background for feature detectors and analyzes their performance robustness in practical implementations. Digital implementation and experimental setup for its performance measurements are described in section 3. In section 4, we describe three experiments using the testbed including detector performance in the presence of sampling offsets, required detection time in highly negative SNRs, and robustness to out-of-band interference. Summary of the work and conclusions are presented in Section 5.

## II. CYCLOSTATIONARY FEATURE DETECTOR

### A. Theoretical Background

Modulated signals are in general coupled with sine wave carriers, pulse trains, repeating spreading, hopping sequences, or cyclic prefixes which result in built-in periodicity. Even though the data is a wide-sense stationary random process, these modulated signals are characterized as *cyclostationary*, since their statistics, mean and autocorrelation, exhibit

periodicity. This periodicity is introduced intentionally in the signal format so that a receiver can exploit it for: parameter estimation such as carrier phase, pulse timing, or direction of arrival. This information can then be used for detection of a random signal with a particular modulation type in a background noise and other modulated signals.

Common analysis of wide-sense stationary random signals is based on autocorrelation function and power spectral density. On the other hand, cyclostationary signals exhibit correlation between widely separated spectral components due to spectral redundancy caused by periodicity. By analogy with the definition of conventional autocorrelation, one can define spectral correlation function (SCF):

$$S_x^\alpha(f) = \lim_{T \rightarrow \infty} \lim_{\Delta t \rightarrow \infty} \frac{1}{\Delta t} \int_{-\Delta t/2}^{\Delta t/2} \frac{1}{T} X_T(t, f + \alpha/2) X_T^*(t, f - \alpha/2) dt \quad (1)$$

where finite time Fourier transform is given by:

$$X_T(t, f) = \int_{t-T/2}^{t+T/2} x(u) e^{-j2\pi fu} du \quad (2)$$

Unlike power spectrum density, which is real-valued one dimensional transform, the spectral correlation function is two dimensional transform, in general complex-valued and the parameter  $\alpha$  is called cycle frequency. Power spectral density is a special case of a spectral correlation function for  $\alpha=0$ .

The sufficient statistics used for the detection are obtained through non-linear squaring operation. Therefore, cyclostationary detectors fall in the category of non-coherent detectors in terms of detection time requirements. Given  $N$  samples divided in blocks of  $T_{FFT}$  samples, spectral correlation function is estimated as:

$$\tilde{S}_x^\alpha(f) = \frac{1}{N} \frac{1}{T} \sum_{n=0}^N X_{T_{FFT}}(n, f + \frac{\alpha}{2}) X_{T_{FFT}}^*(n, f - \frac{\alpha}{2}) \quad (3)$$

$X_{T_{FFT}}(n, f)$  is the  $N_{FFT}$  point FFT around sample  $n$ .

### B. Robustness Issues

Given that feature detectors exploit additional coherency in the signal that is not present in noise, the natural question arises if there are robustness issues involved in the detector performance. In cyclostationary processing of the features related to the symbol clock, it is evident that sampling of the incoming signal becomes critical. Intuitively, random sampling of a periodic signal would not resemble its periodicity. Features are easily recovered if the sampling clock is an integer multiple of symbol rate. However, if there is a sampling clock offset there will be a progressive drift in the position of sampling points within a symbol time. This drift changes the spectral correlation function. First, note that a constant time offset introduces a phase offset in both frequency and spectral correlation function domain.

$$\bar{x}(t) = x(t - t_0) \xrightarrow{F} \bar{X}(f) = X(f) e^{-j2\pi f t_0} \quad (4)$$

$$\bar{S}_x^\alpha(f) = S_x^\alpha(f) e^{-j2\pi \alpha t_0} \quad (5)$$

Since SCF is a complex function, a time offset has different effect on it than on a power spectrum density, which is a real function. Now assume that there is a residual sampling clock offset  $\Delta$  from the ideal sampling clock  $T_0$ , i.e.  $T - T_0 = \Delta$  where  $T$  is the sampling clock interval. Then, in the process of estimation of SCF every estimate obtained by correlation of FFT bins will have a phase offset. Let us assume that  $N$  FFTs are used to estimate SCF as

$$\tilde{S}_x^\alpha(f) = \frac{1}{N} \sum_{i=1}^N \bar{S}_x^\alpha(i, f) \quad (6)$$

where each FFT serves to estimate

$$\bar{S}_x^\alpha(i, f) = \frac{1}{T_{FFT}} X_{T_{FFT}}(i, f + \frac{\alpha}{2}) X_{T_{FFT}}^*(i, f - \frac{\alpha}{2}) \quad (7)$$

Now, in the presence of clock offset estimations, each FFT block will have a phase offset:

$$\bar{S}_x^\alpha(i, f) = \frac{1}{T_{FFT}} \bar{X}_{T_{FFT}}(i, f + \frac{\alpha}{2}) \bar{X}_{T_{FFT}}^*(i, f - \frac{\alpha}{2}) \quad (8)$$

$$\bar{S}_x^\alpha(i, f) = S_x^\alpha(i, f) e^{-j2\pi \alpha t_i} \quad (9)$$

Where  $t_i = iN_{FFT}\Delta$  and  $S_x^\alpha(i, f)$  is the estimate with perfect sampling. In the process of averaging, these estimates are non-coherently added and resulted SCF has the attenuated feature:

$$\begin{aligned} \tilde{S}_x^\alpha(f) &= \tilde{S}_x^\alpha(f) \sum_{i=1}^N e^{-j2\pi \alpha t_i} \\ \tilde{S}_x^\alpha(f) &= \tilde{S}_x^\alpha(f) \frac{\sin(2\pi \alpha \Delta N_{FFT} N / 2)}{\sin(2\pi \alpha \Delta N_{FFT} / 2)} e^{-j2\pi \alpha \Delta N_{FFT} (N+1) / 2} \end{aligned} \quad (10)$$

The feature at  $\alpha$  can be completely cancelled when  $\Delta \approx 1/(\alpha N N_{FFT})$ . Sampling offset  $\Delta$  can be expressed in terms of sampling clock frequency offset  $\delta$  as

$$\Delta = \frac{\delta}{\alpha(\alpha - \delta)} \quad (11)$$

Similar to the coherent pilot detector case, the number of samples that can be used for sensing is limited to

$$N N_{FFT} < \frac{\alpha}{\delta} \quad (12)$$

The cancellation of the features due to sampling clock offset can be prevented by performing partially coherent feature processing. Based on the maximum expected sampling offset  $\delta_{max}$ , number of coherent averages  $M_l$  is chosen to be  $\alpha/\delta_{max} N_{FFT}$ . Then two stage processing is performed as:

$$S_x^\alpha(f)' = \frac{1}{T_{FFT}} \sum_{m=1}^{M_l} \left| \sum_{k=1}^{M_l} X(k + mM_2, f + \frac{\alpha}{2}) X(k + mM_2, f - \frac{\alpha}{2})^* \right|$$

where the total number of averages is  $N = M_l M_2$ .

### C. Feature vs. Signal Energy

The performance of the feature detector also depends on how much energy a feature contains. Different modulation schemes have different features and energy associated with them. Here, we will take a common example of a class of amplitude modulated signals and analyze the feature associated with the symbol rate. All amplitude modulated signals can be represented as:  $x(t) = \sum_{n=-\infty}^{\infty} a_n q(t - nT_s)$  where  $a_n$  is

data sequence,  $q(t)$  is a pulse shaping filter and  $T_s$  is a symbol rate.

The cyclic spectrum of  $x(t)$  is given by:

$$S_x^\alpha(f) = \frac{1}{2T_s} Q(f + \frac{\alpha}{2}) Q(f - \frac{\alpha}{2})^* \text{ for } \alpha = 1/T_s \quad (13)$$

where  $Q(f)$  is a pulse shaping filter in Fourier domain. In case of most commonly used square root raised cosine filter, the feature spans over

$$\frac{1-\beta}{2T_s} < f < \frac{1+\beta}{2T_s} \quad (14)$$

where  $\beta$  is a roll-off factor of the square root raised cosine filter. Since filters with  $\beta=0$  are not realizable, every practical system will have some energy in the feature. Larger  $\beta$  contributes to a larger spectrum redundancy and would provide larger energy in the feature.

## III. IMPLEMENTATION AND EXPERIMENTAL SETUP

In order to study performance and robustness issues of the feature detector, we used the wireless testbed built around Berkeley Emulation Engine (BEE2) [2]. This testbed also allowed us to investigate low complexity implementations of feature detectors.

### A. Experimental setup

The detection of signal features and investigation of detector robustness to sampling offsets require real-time experiments. However, feature detection involves complex signal processing with high computational requirements that must be performed at the high speed sampling clock. The BEE2 processing engine, used in our experimental study, was particularly suitable as it can support up to 500 GOPS at 100 MHz rate. Furthermore, it is an FPGA based platform that allows VLSI implementation and reconfiguration during a run time. Wireless experiments are performed using 2.4 GHz radios front-ends so that real noise and interference sources are incorporated.

### B. Detector Architecture

Implementation of the cyclostationary feature detectors requires computation of spectral correlation function. The frequency domain estimation methods require computation of an  $N_{FFT}$  point FFT plus a cross-correlation of all bins and averaging over a period of detection time. However, for the specific signal of interest only the deterministic region of SCF needs to be computed. Therefore, the multiplication intensive cross-correlation can be limited to the frequency bins occupied by a signal of interest. We developed a parametrizable architecture for computation of any segment of  $N_{FFT}$  by  $N_{FFT}$  matrix representing SCF. Figure 1 shows the detailed block diagram. In order to match input rate of  $N_{FFT}$  samples and output rate of a maximum  $N_{FFT}^2$ ,  $K$  frames ( $K < N_{FFT}$ ) are buffered and arranged so that cross-correlation could be performed through a simple scalable data path of multiplexers, delay lines, and multipliers. We implemented a 256 pt. FFT and computed SCF of size  $256 \times 16$  ( $N=256$ ,  $K=16$ ). The implementation complexity is compared with 256 pt. FFT energy detector and  $K=32$  cyclostationary detector. Design summaries are reported in Table 1. The number of

multiplications increases by an order of magnitude with respect to energy detector. If the computation of the entire SCF (256x256) is required, the number of multipliers would increase to 1044. The proposed implementation is scalable to any  $K$  being power-of-two number in the range from 1 to 256.

In order to increase detector robustness to sampling offsets we implemented a two stage SCF averaging as proposed in Section II-B. The first stage averages SCF in the complex domain so that features are coherently added and the noise is cancelled. The second stage averages magnitude of the output of the first stage, and therefore it changes the processing from coherent to non-coherent. The output of the detector is obtained through integration of the energy in the SCF that lies in  $(\alpha, f)$  where signal of interest has theoretically predicted features. This integration is implemented using a software programmable mask. In addition, the number of averages for both stages  $M_1$  and  $M_2$  are controllable through software at the run time.

#### IV. EXPERIMENTAL RESULTS

Our experimental study investigates the following:

- A. Sensitivity of feature detectors to sampling clock offsets
- B. Performance of the proposed feature detector
- C. Comparison of the feature detector and energy detector in the presence of out-of-band interference

##### A. Sensitivity to sampling offsets

The signal of interest is a 4 MHz QPSK signal upconverted to ISM band at 2.485 GHz, and generated by a standard vector signal generator. A baseband pulse shaping filter is a square root raised cosine with the roll-off  $\beta=0.5$ . The transmitter and receiver are connected through a SMA cable in order to emulate AWGN channel. The receiver down-converts the signal to low IF and samples it using A/D converters at 64 MHz with 12 bits resolution. The A/D sampling clock is fed externally and can be programmed with the desired frequency offset. Expected feature of the QPSK signal related to the symbol clock corresponds to  $\alpha=4$  MHz. Figure 2a shows the 2 dimensional SCF with perfect sampling. Number of averages in the first stage  $M_1=1000$ . The diagonal trace correlates each FFT bin with itself, thus represents the power spectrum density (PSD) of the signal and can be used for energy detection. The distinct feature related to  $\alpha=4$  MHz is located on the off-diagonal at 4MHz distance from the main diagonal. The energy of the feature as well as its width in SCF is related to the 0.5 filter roll-off factor. Next, we introduce  $\delta=100$  Hz

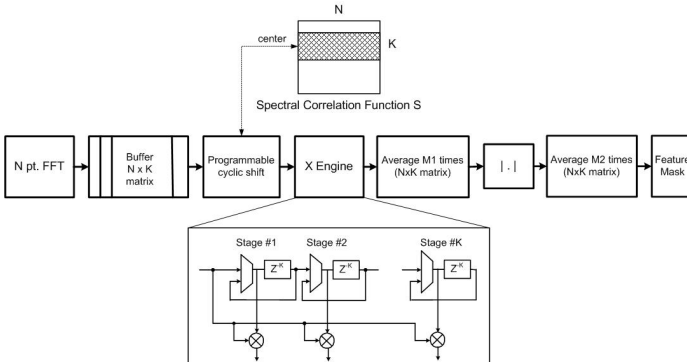


Figure 1. Flexible implementation of feature detector robust to sampling offsets

Resources	Energy Detector	Feature Detector (K=16)	Feature Detector (K=32)
18x18 Mult	18	82	162
16 Kb Block RAM	4	83	165
4 input LUT	10,353	21,200	24,389
Flip Flop	12,155	20,559	23,609

Table 1. Implementation complexity comparison

offset to a 64 MHz sampling clock. In this experiment, we used only the first stage averaging and kept  $M_1=1000$ . Figures 2b shows the estimated SCF under these conditions. As expected, cyclostationary features of the signal are cancelled out. This result shows that feature detectors are highly sensitive to sampling offset. If the offset is not corrected, the feature detector will fail even in highly positive SNRs.

##### B. Feature detector performance

The proposed feature detector with 2 stage averaging (Figure 1) is expected to overcome the sampling clock offset issues. Now, the question is what the performance degradation with respect to perfect sampling is. In addition, we were interested to compare this detector with a simple energy detector in highly negative SNR regimes. Our interest was to explore if this scheme could be used for robust spectrum sensing in cognitive radios.

We measured the required sensing time to meet probability of detection of 80% and probability of false alarm of 10% for SNRs between -9 and -21 dB. The experimental methodology is the same as in [3]. The number of FFT averages corresponds to a product of number of averages in stage 1 and stage 2. Figure 3 presents the measurement results. Under stationary white noise, feature detectors (even with perfect sampling) have a performance loss with respect to energy detector. This is due to the fact that energy contained in the feature is related to the pulse shaping filter roll-off, as described by Eq. 13. In case of  $\beta=0.5$  the loss is approximately 6 dB. On the other hand, a sampling clock offset of 100 Hz at 64 MHz makes the detection of signals below -15 dB SNR impossible. However, once the proposed 2 stage averaging is deployed the detector achieves the desired probability of detection and false alarm at the penalty of increase detection time. The number of averages in the first stage is chosen from the Eq. 12. For SNRs below -15 dB, the number of averages in

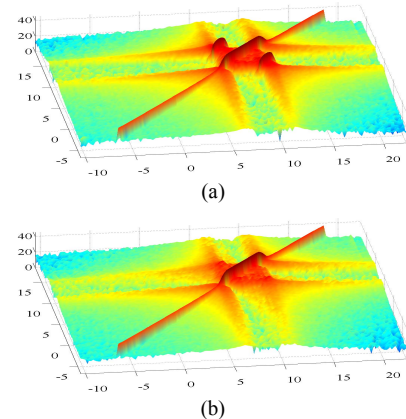


Figure 2. SCF of 4 MHz QPSK signal a) with perfect sampling, b) with 100 Hz sampling offset

the second stage has to be increased with respect to perfect sampling feature detection. The proposed scheme performs comparable even for sampling offsets of 1 KHz. As a result, the proposed feature detection in the presence of sampling clock offsets can be used for reliable weak signal detection, but the required detection time is significantly larger than energy detection. Note, that this results hold only for stationary white noise.

### C. Robustness to out-of-band interference

It has been shown that energy detector is highly susceptible for the noise variance uncertainty that is contributed by temperature variations and out-of-band interference [3]. To test the robustness of feature detectors, we experiment with the adjacent channel interference coming from the commercial 802.11g WLAN with a continuous traffic generated by video camera data transfer between two laptops. The interference scenario in feature domain is presented in Figure 4.

Figure 5 shows the performance of both energy and feature detectors in the presence of adjacent band interference. Due to spectral leakage of the FFT, energy detector suffers from the large variation in the noise-plus-interference level. This variation progressively degrades the energy detector performance and at -18dB SNR detection becomes impossible. On the other hand, feature detector robustly detects the weak signals and outperforms the energy detector. Note that there is a slight degradation in performance of feature detector as well due to leakage of the interference signal in SCF domain. We are currently investigation windowing techniques that can suppress this effect.

### V. CONCLUSIONS

In this paper we present the complete characterization of cyclostationary feature detectors through theoretical analysis, implementation, and experiments under real noise and interference sources. The real-time system implementation allowed us to identify the robustness issue of feature detectors with respect to sampling clock offsets. This effect has been ignored in all theoretical and simulation studies of the cyclostationary signal detection so far. We proposed the 2 stage averaging scheme to overcome the feature cancellation due to sampling offsets. Measurement results quantified the performance degradation, but also showed that detector can be

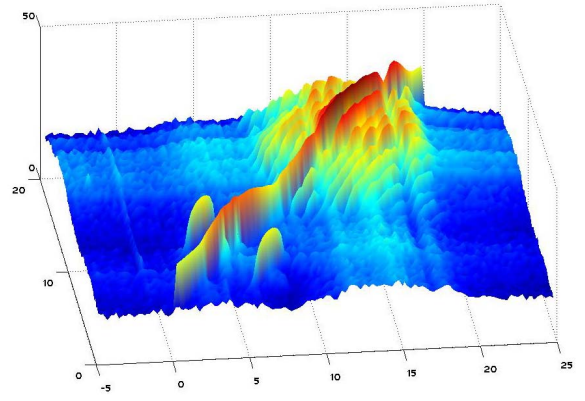


Figure 4. Features of desired QPSK signal and the adjacent 802.11g signal

used in highly negative SNRs. In addition, we compared the proposed feature detector with the conventional energy detector. In stationary noise channels, feature detectors are inferior since the energy in the feature is always smaller than the total energy of the signal. However, in the presence of strong adjacent channel interferers noise becomes non-stationary. Then, the energy detector fails to detect weak signal while feature detector is not affected.

### VI. ACKNOWLEDGEMENTS

This work has been supported by MARCO fund (C2S2) under contract 2003-CT-888 and BWRC industry members.

### VII. REFERENCES

- [1] W.A.Gardner, "Signal Interception: A Unifying Theoretical Framework for Feature Detection", IEEE Trans. on Communications, vol. 36, no. 8, August 1988
- [2] C. Chang, J. Wawrzyn, and R. Brodersen, "BEE2: A High-End Reconfigurable Computing System", in Proc. of IEEE Design and Test of Computers, March 2005.
- [3] D. Cabric, A. Tkachenko, R. W. Brodersen, "Spectrum Sensing Measurements of Pilot, Energy and Collaborative Detection", in Proc. of IEEE Military Communications Conference, Oct. 2006

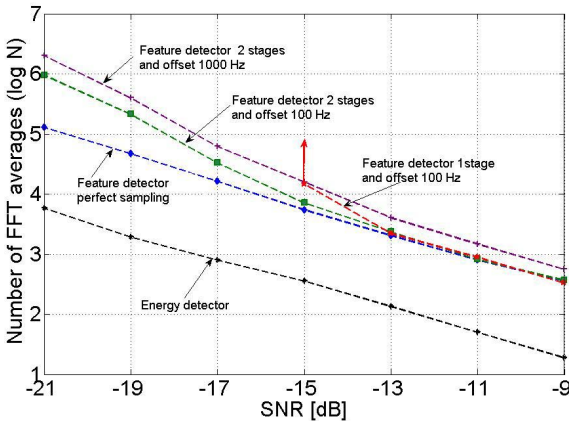


Figure 3. Detection time vs. SNR comparison for energy and feature detectors in AWGN

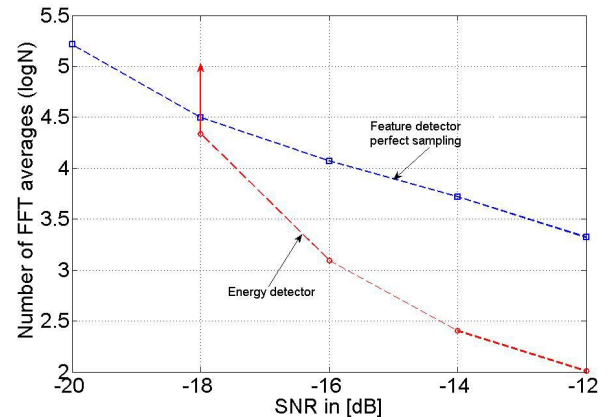


Figure 5. Detection time vs. SNR comparison for energy and feature detectors in the presence of out-of-band interference